

A Constitutive Model for Blended Yarn Extension with Fragmented Low-Elongation Fibers

THOMAS A. GODFREY

Natick Soldier Center, U.S. Army Soldier & Biological Chemical Command, Natick, Massachusetts 01760, U.S.A.

JOHN N. ROSSETTOS

*Department of Mechanical, Industrial & Manufacturing Engineering,
Northeastern University, Boston, Massachusetts 02115, U.S.A.*

ABSTRACT

A simple micromechanical model is developed for the interactions in a parallel square-stacked mixed array of elastic fibers representing the microstructure of a blended yarn undergoing axial extension. The mixed array consists of a small fraction of relatively high modulus, low elongation-to-break (LE) fibers dispersed among high elongation-to-break (HE) fibers. The LE fibers are assumed to break into fragments, and the LE fiber fragments are assumed to slip relative to neighboring fibers in regions near the fragment tips. The fiber array experiences lateral compression arising from the remote tension on the twisted yarn, and frictional forces acting at slipping fiber-to-fiber contact surfaces are assumed to obey Amontons' law. Solutions of a dimensionless boundary value problem for deformations in a unit cell of the fiber array are presented. Dimensionless parameters involving the constituent LE and HE fiber properties are identified and their influence on blended yarn tensile behavior is illustrated.

Blended or *hybrid* yarns, consisting of two different fiber types, have long been produced to improve strength, stiffness, and other qualities over what can be achieved in homogeneous yarns. Often a stiff, low elongation (LE) fiber is combined with a compliant, high elongation (HE) fiber to obtain a yarn with both high initial stiffness and high elongation-to-break. During extension of such yarns, there is a fragmentation process where the LE fiber develops multiple breaks along its length [12, 16]. A similar process occurring in hybrid composites is believed to be an important factor in realizing desirable hybrid effects [14, 19]. First, a series of isolated breaks develop along the LE fibers. Because the nominal strain in the neighborhood of the LE fibers increases, intermediate breaks occur, such that the LE fibers are broken into fragments with an identifiable average length. With continued extension, the fragments develop additional breaks, and so the fragment size becomes progressively smaller. A beneficial hybrid effect is achieved when conditions permit the LE fiber fragments to continue to contribute to the overall stiffness and load-carrying ability of the yarn.

Twisted fibrous structures, including yarns, ropes, and cables, exhibit a unique and important behavior when loaded in tension. Due to the yarn's twisted geometry, transverse compressive forces are induced by the remote tension along the yarn axis. Each fiber executes a quasi-helical path through the yarn and so requires a radially outward-directed distributed reaction force from underlying fiber layers to balance the tension on the curved fiber element. Transverse compressive forces permit load transfer to occur between abutting fibers through friction and give the yarn the cohesiveness needed to function as a structural unit. With increasing yarn tension, transverse compressive forces also increase, therefore increasing the magnitude of frictional load transfer between fibers. This mechanism, first recognized by Galileo [5], is particularly important in structures twisted from short plant and animal fibers (*i.e.*, staple yarns), which rely entirely on friction for structural integrity. In this work, the induced transverse compressive forces play a crucial role by governing, through Amontons' law, the magnitude of frictional forces at slipping contact surfaces between LE fiber fragments and HE fibers.

Analytical works on the mechanics of continuous filament yarns fall in two major areas, stress analysis and strength prediction. There is extensive literature on yarn stress analysis: representative works include those of Hearle [7, pp. 175–212], Kilby [13], and Thwaites [25, 26]. Generally, these works treat a helical element of the twisted yarn, parallel to the local filament direction, as a continuum with a variety of simplifying assumptions for the constitutive behavior of the packed fibers. As such, yarn stress analysis is concerned with deformations that may be considered homogeneous over a large number of fibers, and so no attention is given to problems of broken fibers. However, in our work, the results for yarn internal stresses obtained in these studies motivate the model used here for frictional load transfer at slipping fiber contact surfaces.

The body of work on strength prediction has emphasized the stochastic aspects of the failure process, beginning with the well-known works of Daniels [3] and Pierce [22]. More recent contributions in this line of research include Phoenix [20], Pitt and Phoenix [23], and Realf *et al.* [24]. These works are intimately concerned with the progression of breaks in discrete fibers; however, with the exception of the work by Pitt and Phoenix [23], mechanical interactions among the fibers are addressed by adopting ad hoc load-sharing rules, such as nearest-neighbor or equal load sharing. Pitt and Phoenix [23] adopted a micromechanical approach to modeling load sharing among fibers in nonhybrid yarns during the failure process. Their approach was based on the classical elastic shear-lag analysis of fiber/matrix composites [8, 9]. The model we have developed in this paper has a mathematical structure similar to Hedgepeth and Van Dyke's [9] shear-lag model for a three-dimensional fiber composite. In the composite case, load transfer takes place by shear of the matrix phase. For packed fiber arrays in hybrid yarns, load transfer occurs through geometry changes in the fibers and surface friction.

Realf *et al.* [24] have made an important contribution to understanding the failure process in blended yarns. Their recent stochastic modeling work illustrates the complex and critical influence of twist-induced transverse compression on the failure process in blended yarns. As previously mentioned, transverse compression strongly influences fiber-to-fiber load transfer, and therefore, the distribution of fiber tensions near a fiber break. In Realf *et al.*'s stochastic model [24], the distribution of tension near a break along the fibers' length axes enters into the model through a *critical length* or *characteristic distance* [23] over which fiber tensions are locally affected by the presence of the break. The critical length is assumed inversely proportional to the lateral

compressive stress. The magnitude of the tensions redistributed to the surviving fibers in a yarn cross section containing one or more fiber breaks is governed by a load-sharing rule that imposes more severe loads on surviving fibers near the break for higher values of yarn twist. By successfully simulating the experimental results of Monego and Backer [15, 16], Realf *et al.* demonstrated that their model, incorporating a reasonable, albeit ad hoc, treatment of fiber-to-fiber mechanical interactions, shows promise for predicting the global response of blended yarns. Our ongoing research, aimed broadly at the basic mechanics of fiber-to-fiber interactions in blended yarns, will prove useful in developing and refining simulation models for the blended yarn failure process.

Developing statistical theories for the mechanical behavior of fibrous composites has been, and continues to be, an active research area. Recent works by Curtin [1, 2], Neumeister [18], Phoenix *et al.* [21], and Hui *et al.* [10] exemplify the high level of sophistication attained in the treatment of complex mechanistic aspects without resort to Monte Carlo simulation. Aspects of modeled behavior include fiber fragmentation, frictional slip of fibers, matrix cracking, fiber pullout during failure, and matrix yielding. Suitable modification of these works to address blended yarn behavior, using the results and insights attainable through our approach, should provide for the eventual development of predictive theories for stress-strain and strength behavior in blended yarns. Such theoretical developments, if pursued, have an advantage over simulation studies in advancing fundamental understanding. Trends in yarn behavior will emerge clearly as functions of the underlying fiber properties.

In this paper, we develop a micromechanical model for the extension of a hybrid fiber array representing the microstructure of a hybrid yarn undergoing fragmentation of the LE fibers. The parallel square-stacked mixed array of elastic fibers consists of a small fraction of relatively high modulus LE fibers dispersed among HE fibers. The LE fibers are assumed to break into fragments that slip relative to neighboring fibers in regions near the fragment tips; analysis of frictional slip forces acting in the slip region is motivated by results for yarn internal stresses [7, pp. 175–212]. We use the model to investigate the contribution of LE fragments to the load-carrying ability of the fiber array. A dimensionless parameter Q , which involves the elastic and frictional properties of the fibers as well as yarn geometry, has a critical influence over the degree to which the behavior of the fiber array is dominated by either elastic or frictional slip effects.

Micromechanical Model

GENERAL DEVELOPMENT—NO SLIP BETWEEN FIBERS

We consider a uniformly blended twisted hybrid yarn composed of a small fraction of LE fibers dispersed among HE fibers. The yarn is assumed to possess a well accepted, idealized, helical structure [7, pp. 65–67] where the fibers lie in co-axial concentric layers and follow helical paths. The tangent of the helix angle varies linearly with radial position in the yarn from zero at the center to a maximum on the yarn surface. Directing our attention to the central region of the yarn, the fibers are nearly parallel to the yarn axis. Fibers near the yarn's center therefore experience the highest strains during yarn extension, and yarn rupture usually initiates in the central region.

Stacking of fibers within twisted yarns is, of course, imperfect. As yarn tension increases, lateral compression drives the local stacking toward a regular periodic structure, *i.e.*, square or hexagonal packing. However, fiber migration and the tendency for the twisted yarn under tension to assume a circular cross section necessitate that the fiber array deviate from a perfect lattice through packing flaws. Size and shape differences between LE and HE fibers in blended yarns are expected to increase the degree of defects in the fiber packing. Hexagonal packing, where each fiber interacts directly with six neighbors, represents the most densely packed configuration of parallel fibers. In square packing, each fiber interacts directly with only four neighbors. Since flaws reduce the overall density of the fiber packing, and the number of nearest-neighbor fibers available for interaction, we regard square packing as providing an effective model for predicting the behavior of real fiber packing within yarns.

We require the cross-sectional dimensions of the LE and HE fibers to be roughly similar to the extent that square packing can be approximated. In common cotton/polyester blends, where the polyester staple may typically be 0.33 tex versus, say, 0.2 tex for the cotton fiber, the roughly elliptical shape of the cotton fiber means the major diameter of the cotton is somewhat larger than the polyester. For example, assuming an aspect ratio of two for the typical cotton fiber, the major diameter of the typical fiber will be 10% larger, and the minor diameter will be 45% smaller, than the diameter of the polyester fiber. Since in the array, the cotton fiber cross sections are randomly oriented about their length axes, we expect that the disturbance caused by their elliptical shapes will average out over a large region containing many cotton fibers. As such, square packing is still a reasonable model despite the sizable size and shape differences. The

commercial success of cotton/synthetic blends suggests that effective packing, key to the structural integrity of the yarn, is indeed attained in practice.

Consider a square-stacked mixed array of parallel, linearly elastic fibers representing the microstructure of the yarn near the yarn's center. For hybrid yarns containing sufficiently small fractions of LE fibers, we assume the LE fibers are far enough apart that their regions of influence do not overlap. The LE fibers are assumed to develop evenly spaced breaks such that they form fragments of uniform length $2l$. Based on these assumptions, we investigate the behavior of a finite section of the fiber array of length l consisting of one-half of a single LE fiber fragment embedded in the center of a square region of HE fibers. This finite section is essentially a unit cell of the fiber array. The x -coordinate axis is parallel to the fiber direction, with the origin placed at an LE fragment tip. The LE and HE fibers are assumed to be approximately transversely isotropic. The fibers are numbered (n, m) , where n is the column number and m is the row number; the center LE fiber is designated $(0, 0)$ (Figure 1). The fiber array is extended in the x -direction to a nominal strain ϵ .

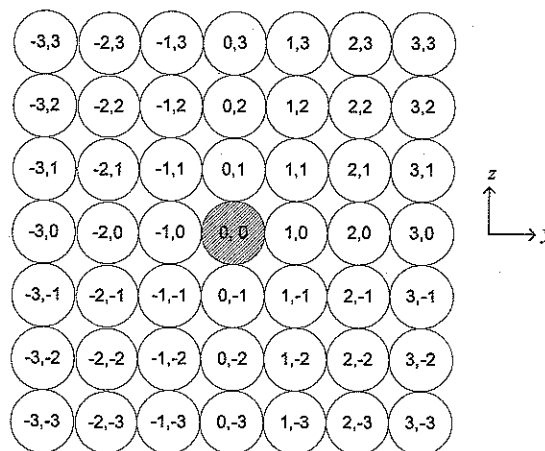


FIGURE 1. Numbering scheme for finite section of fiber array. LE fiber shown shaded.

The general form of the fiber equilibrium equation in the square-stacked array can be derived as follows: Consider the n, m th fiber and its abutters. The fiber array is laterally compressed, due to the interaction of yarn tension and twist, so that fiber-to-fiber load transfer may occur by means of surface friction. Along the contact line with each of its four abutters, a contact "shear flow" is applied to the n, m th fiber. The term *shear flow* is used here to connote a force per unit length. Figure 2 illus-

trates the shear flows and their contributions to axial equilibrium of the n, m th fiber. HE fibers each have an effective axial stiffness E^*A^* , and the LE fiber has an effective axial stiffness EA . In the notation for the shear flows, superscripts denote the row numbers and subscripts denote the column numbers, e.g., $q_i^{j,j+1}$ is the shear flow between fibers in column i , rows j and $j+1$. Introduce $u_{n,m}$ as the average axial (x -direction) displacement in fiber (n, m) at position x . It is convenient to take as the displacement reference the position of points on an undamaged fiber array (the LE fiber is not fragmented) under the same nominal strain. For HE fibers, the axial force due to LE fiber fragmentation is $E^*A^*(du_{n,m}/dx)$. From the free body diagram, Figure 2c, axial equilibrium can therefore be written as

$$E^*A^* \frac{d^2 u_{n,m}}{dx^2} + q_{n,n+1}^m - q_{n-1,n}^m + q_n^{m,m+1} - q_n^{m-1,m} = 0 \quad (1)$$

Our goal is to develop a simple, semi-empirical model involving a minimum number of physical parameters, some of which will ultimately be calibrated using experimental data. With this in mind, we propose that, given that no slip occurs at the contact surface, the shear flow at the contact line between two abutting fibers may be considered linearly proportional to the difference in the fibers' average axial displacements. For a contact line between an HE fiber and the LE fiber, we denote the proportionality constant k , and use k^* for contact lines between two HE fibers. When fiber (n, m) and all its abutters are HE fibers, we may write the shear flows on fiber (n, m) as

$$\begin{aligned} q_{n,n+1}^m &= k^*(u_{n+1,m} - u_{n,m}) \quad , \\ q_{n-1,n}^m &= k^*(u_{n,m} - u_{n-1,m}) \quad , \\ q_n^{m,m+1} &= k^*(u_{n,m+1} - u_{n,m}) \quad , \\ q_n^{m-1,m} &= k^*(u_{n,m} - u_{n,m-1}) \quad . \end{aligned} \quad (2)$$

The proportionality constants k and k^* involve shearing of fibers longitudinally due to surface tractions along the fiber-to-fiber contact lines. Treating the fiber material as a homogenous solid, the stiffness constant k^* will be proportional to the HE material's shear modulus in the longitudinal transverse plane G_{LT} . The constant k will involve the shear moduli of both fibers in a springs-in-series arrangement. Measurements of the shear modulus of a variety of textile fibers are tabulated in the book by Morton and Hearle [17, pp. 418 and 428]; they range from 0.33 to 1.6 GPa. Physical reasoning suggests the value of k^* should be somewhat less than the value of G_{LT} for the HE fiber material, since the packed array of HE fibers may be regarded as a porous solid.

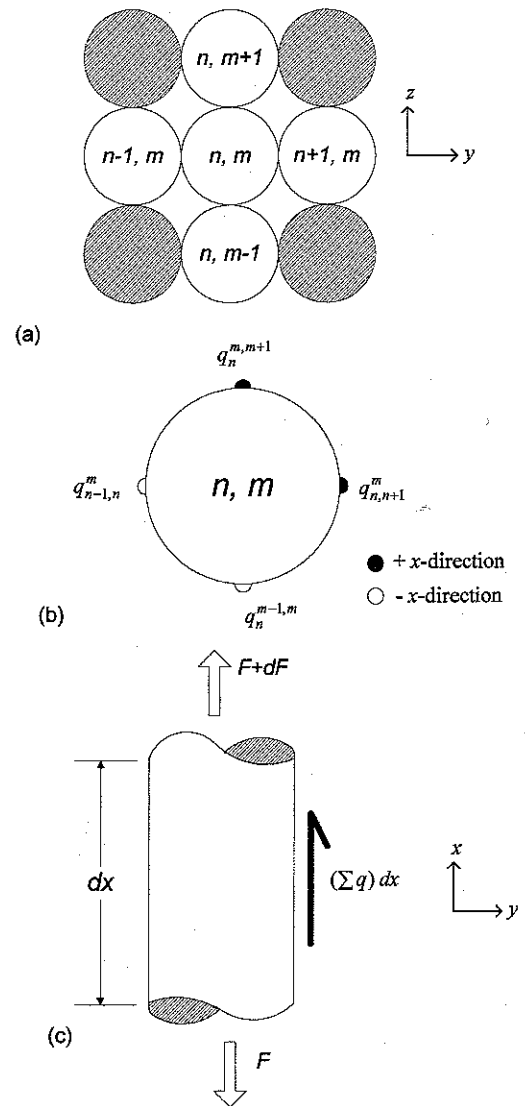


FIGURE 2. (a) n, m th fiber and abutters, (b) contact line shear flows, (c) n, m th fiber free body diagram.

The dimensionless position coordinate ξ and displacements $U_{n,m}$ are defined by

$$x = \sqrt{E^*A^*/k^*} \xi, \quad u_{n,m} = \varepsilon \sqrt{E^*A^*/k^*} U_{n,m} \quad (3)$$

Putting Equations 2 into Equation 1 and nondimensionalizing, using Equations 3, the dimensionless equilibrium equation for fiber (n, m) is written as

$$U''_{n,m} + U_{n+1,m} + U_{n-1,m} + U_{n,m+1} + U_{n,m-1} - 4U_{n,m} = 0 \quad (4)$$

where primes denote differentiation with respect to ξ .

For the center LE fiber and the HE fibers abutting that LE fiber, the equilibrium equations take a slightly different

form. For LE fiber (0, 0), following the previous procedure, we write

$$EA \frac{d^2 u_{0,0}}{dx^2} + q_{0,1}^0 - q_{-1,0}^0 + q_0^{0,1} - q_0^{-1,0} = 0 \quad (5)$$

Using our constitutive assumption relating shear flows and displacements, taking into account symmetry in the deformation ($u_{1,0} = u_{0,1} = u_{-1,0} = u_{0,-1}$), and nondimensionalizing, using Equations 3, we obtain

$$U''_{0,0} + 4 \frac{E^* A^*}{EA} \left(\frac{k}{k^*} \right) (U_{1,0} - U_{0,0}) = 0 \quad (6)$$

The HE fiber (1,0) abuts the LE fiber and three other HE fibers. The dimensionless equilibrium equation for fiber (1,0), considering symmetry, is

$$U''_{1,0} + U_{2,0} + 2U_{1,1} + \frac{k}{k^*} U_{0,0} - \left(3 + \frac{k}{k^*} \right) U_{1,0} = 0 \quad (7)$$

FRICIONAL SLIP IN THE FRAGMENTED FIBER ARRAY

As previously mentioned, there is extensive literature on internal stresses in twisted yarns during extension. Generally, workers have assumed that radial and circumferential compressive stresses are equal, arguing that fibers are free to slide over each other laterally—exhibiting fluid-like behavior. Authors often refer to the lateral stress as a lateral hydrostatic pressure. For most of the interior of the yarn, the assumption of equal radial and circumferential compressive stress components should be a fairly good approximation. In this paper, we adopt a simple phenomenological description that is compatible with the literature [7, pp. 175–212]. The fiber array is assumed to experience a laterally “hydrostatic” stress, $\sigma_y = \sigma_z = \sigma$. Here, however, we use engineering stress, with dimensions of force/(length)², rather than the specific stress (force/linear density) commonly used in the textile literature. The lateral and axial stresses are average stresses in a continuum that includes the packed fibers and the voids between them. The magnitude of the lateral stress is assumed equal to the product of the axial stress in the fiber array σ_x and a function η of yarn surface helix angle and radial position of the fiber array within the yarn. As a first-order approximation, we take the axial stress equal to the axial stiffness of the fiber array \bar{E} times the nominal axial strain ($\sigma_x \gg |\sigma|$). Therefore, the lateral stress is written as

$$\sigma \cong -\bar{E}\varepsilon\eta \quad (8)$$

For estimating a magnitude of η , Hearle’s results [7, pp. 175–212] can be used, where our η is analogous to his normalized lateral stress g when both are evaluated at the

yarn center. Assuming constant volume deformation of the yarn during extension, we may estimate η ’s value near the yarn center as $\eta \cong 0.5 \ln(\cos \alpha) + 0.75 \sin^2 \alpha$, where α is the surface helix angle. For a yarn surface helix angle of 40°, for example, η would be 0.18.

We assume that slip occurs between the LE fragment and the abutting HE fibers in a region near the LE fragment tip, $0 \leq x < a$, where a is less than l . The shear flow acting along each slipping contact line is denoted q_s . Denoting the average fiber spacing as d , the normal contact force per unit length along the fiber-to-fiber contact line is $-d\sigma$, where σ is the average lateral stress in the continuum. Amontons’ law requires that $q_s = -\mu d\sigma$, where μ is the coefficient of friction between slipping LE and HE fiber surfaces. Therefore, using Equation 8, the shear flow along the slipping contact line may be written as

$$q_s = \mu d \bar{E} \varepsilon \eta \quad (9)$$

For the center LE fiber fragment, equilibrium in the slipping region, $0 \leq x < a$, may be written as

$$EA \frac{d^2 u_{0,0}}{dx^2} - 4q_s = 0 \quad (10)$$

where the coefficient 4 arises from the LE fragment slipping against its four HE abutters. Using Equations 3, Equation 10 may be nondimensionalized, giving

$$U''_{0,0} - 4 \frac{E^* A^*}{EA} Q = 0 \quad (11)$$

where Q is given by

$$Q = \frac{q_s}{\varepsilon \sqrt{k^* E^* A^*}} \cong \frac{\mu d \bar{E} \eta}{\sqrt{k^* E^* A^*}} \quad (12)$$

In the second of Equations 12 we have used Equation 9. The parameter Q involves only properties of the constituent fibers, the properties of the smeared fiber array, the position of the array within the yarn, and the yarn twist (through η). Therefore, Q may be regarded as somewhat of a *material property* of the hybrid yarn.

For fiber (1, 0), frictional slip occurs along its contact line with the center LE fragment, but we assume no slip occurs between it and its other three abutters. The dimensionless equilibrium equation may be obtained from the equation for the nonslipping region, Equation 7, by replacing the terms arising from the elastic interaction with fiber (0, 0), $(U_{0,0} - U_{1,0})k/k^*$, with $+Q$, representing the frictional slip shear flow acting on the fiber (1, 0) in the positive x -direction (the LE fragment slips in the $+x$ -direction). Therefore, the equilibrium of fiber (1, 0) may be written as

$$U''_{1,0} + U_{2,0} + 2U_{1,1} - 3U_{1,0} + Q = 0 \quad (13)$$

SYSTEM OF EQUATIONS AND BOUNDARY
VALUE PROBLEM

The finite section unit cell of the fiber array consists of the square region of fibers lying in the rows and columns numbered $-M$ through M . We have assumed that the LE fibers are dispersed far enough apart in the fiber array such that their influence is contained within a finite neighborhood of HE fibers that form a unit cell. Therefore, the fiber-to-fiber shear flows arising from the LE fiber fragmentation are contained within the unit cell, and the unit cell outer boundary is free of any shear flows arising from interactions with fibers lying in the $M + 1^{\text{th}}$ and $-M - 1^{\text{th}}$ row or column. The square region exhibits eight-fold symmetry such that we need only write equations for the $(M + 1)(M + 2)/2$ fibers lying in a right-triangular wedge, as shown in Figure 3 for the case $M = 3$. The equations for the center LE fragment and the abutting HE fiber were developed earlier. Development of the equations for the remaining fibers in the wedge region proceeds from the development of Equation 4, and involves specializing Equation 4 to take into account the shear-free condition on the unit cell outer boundary (for fibers in the M^{th} column) and/or symmetry (for fibers on the wedge boundary). This development is straightforward and will not be given here.

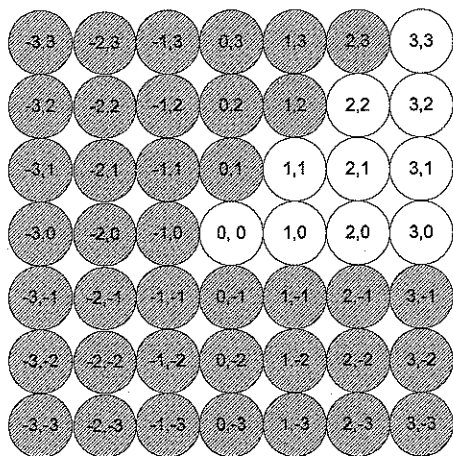


FIGURE 3. Eight-fold symmetry in square array. Equations are written only for the nonshaded fibers in the wedge-shaped region. $M = 3$ for the array shown here.

In real blended yarns, the LE fibers will mix at random with the HE fibers; the LE fibers will not be uniformly dispersed with a set number of HE fibers between them. As such, our square unit cell is not intended to represent a verbatim repeating pattern in a perfect periodic structure. The choice of M is therefore more or less arbitrary,

since M does not depend directly on the specific fraction of LE fibers in a particular blend. It turns out that for the calculations in this paper, choosing M to be 2 or 4 makes an insignificant difference in the results. Our approach should be useful in describing the behavior of blends such that the four immediate abutters of each LE fiber are usually all HE fibers, blends involving up to, say, 10% LE fibers. To address the behavior of blends with higher proportions of LE fibers will require an extension of the current work to consider configurations where an LE fiber is routinely abutted by one or more other LE fibers. Nonetheless, we expect our approach will be useful in predicting trends in blended yarn behavior in general.

The finite section *unit cell* of the fiber array has length l , one-half the length of the LE fragment. The dimensionless length of the unit cell is denoted L , where L is defined by $l = \sqrt{E^*A^*/k^*}L$, using Equations 3. The unit cell represents the repeating pattern of displacements occurring in the fiber array due to LE fiber breaks roughly evenly spaced $2l$ apart. Clearly, $\xi = L(x = l)$ is a plane of symmetry for displacements due to damage, so for all fibers, we write

$$U_{n,m}(L) = 0 \quad (14)$$

At $x = 0$, fiber (0, 0) is stress-free (broken), so using the definition of the displacement reference and Equations 3 leads to

$$U'_{0,0}(0) = -1 \quad (15)$$

In an earlier paper, we developed a boundary condition similar to Equation 15 in more detail (Godfrey and Rossetto [6]). For the intact HE fibers, $\xi = 0$ is also a plane of symmetry; therefore,

$$U_{n,m}(0) = 0, \quad (n, m) \neq (0, 0) \quad (16)$$

Slip occurs between the LE fragment and its HE abutters in the region $0 \leq x < a$, where a is termed the extent of the slip region. The dimensionless slip region extent is denoted α , defined by $a = \sqrt{E^*A^*/k^*}\alpha$, using Equations 3. We divide the unit cell into region I, $0 \leq \xi < \alpha$, where slip occurs along the LE fragment, and region II, $\alpha \leq \xi < L$, where no slip occurs. The system of equations for fiber equilibrium in region I consists of Equations 11, 13, and 4 specialized as needed for each of the remaining fibers in the wedge. In region II, the system includes Equations 6, 7, and 4 specialized as needed for each of the remaining fibers in the wedge. Since all fibers are continuous at $\xi = \alpha$, the following continuity conditions hold, where superscripts I and II refer to the solution in regions I and II, respectively,

$$U_{n,m}^{\text{I}}(\alpha) = U_{n,m}^{\text{II}}(\alpha); \quad U'_{n,m}^{\text{I}}(\alpha) = U'_{n,m}^{\text{II}}(\alpha) \quad (17)$$

An additional continuity condition arises from the assumption that slipping is approached in a continuous fashion—the shear flows on the LE fragment in the non-slipping region approach those in the slipping region as $\xi \rightarrow \alpha$. Using Equations 6 and 11, this condition may be written as

$$Q = \frac{k}{k^*} \{U_{0,0}^{\text{II}}(\alpha) - U_{1,0}^{\text{II}}(\alpha)\} \quad (18)$$

The systems of equations for regions I and II are written in matrix form, and solutions in each region are obtained using an eigenvector expansion technique, as described in detail for a similar boundary value problem [6]. The solution process is completed by selecting values of the slip region extent α and determining the values of the integration constants and parameter Q , such that the boundary and continuity conditions, Equations 14–18, are satisfied.

In the results that follow, the parameter E^*A^*/EA (the ratio of HE to LE fiber axial stiffnesses) is denoted R , after the notation used for a similar parameter in the hybrid composites literature [4]. This parameter occurs in Equations 6 and 11.

Results

SLIP REGION EXTENT

The behavior of the slip region extent with increasing Q for various fragment lengths is exhibited in Figure 4. For the case shown, $R(=E^*A^*/EA) = 1/3$ and $k/k^* = 1$. A value of $R = 1/3$ would be typical for a cotton/nylon staple blended yarn. For fragments of length $L = 2$ and greater, the extent of slip behavior is similar for values of Q greater than, say, 0.4. For this regime of Q values and fragment lengths, the LE fiber breaks are sufficiently far apart that they no longer influence each other, *i.e.*, they appear to be isolated breaks in an essentially infinite fiber. For vanishingly small Q , the slip region extent approaches the fragment length.

The influence of varying the elastic properties of the fiber array on slip extent behavior is exhibited in Figure 5. Increasing the axial stiffness of the LE fragment relative to the HE fibers (decreasing R) increases the slip extent at given values of Q . Increasing the stiffness of the shearing interaction between the LE fragment and the HE fiber (increasing k/k^*) also increases the slip extent at given values of Q .

STRAIN PROFILES

The strain in a particular fiber of the array is $\varepsilon + du_{n,m}/dx$, where the ε (nominal strain) term occurs due to the definition of the displacement reference. In the

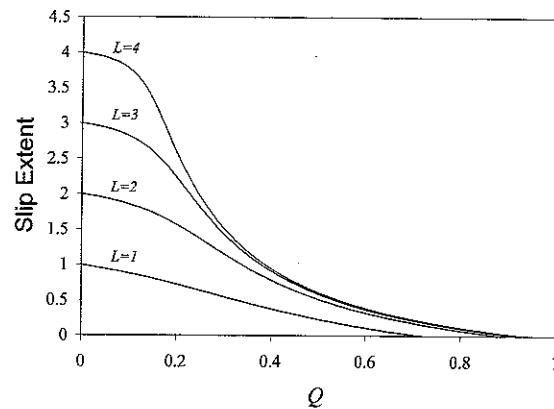


FIGURE 4. Slip extent α versus Q for various fragment lengths, $R = 1/3$, $k/k^* = 1$. Fragment length L shown next to curves.

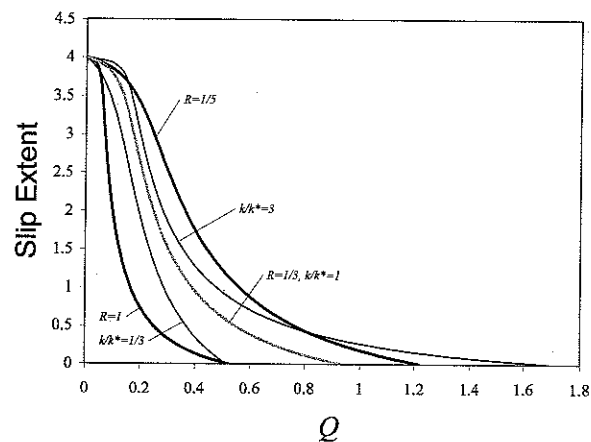


FIGURE 5. Slip extent α versus Q for various R and k/k^* values. For k/k^* equal to $1/3$ and 3, R is $1/3$. For R equal to 1 and $1/3$, k/k^* is 1. Fragment length L is 4 for all cases.

dimensionless variables, fiber strain becomes $\varepsilon(1 + U'_{n,m})$. The strain profiles along the center LE fragment and the abutting HE fiber for various values of Q are exhibited in Figure 6. For this case, $R = 1/3$, $k/k^* = 1$, and $L = 2$. There is a clear trend toward an increasingly linear strain profile with decreasing values of Q for the fragment and the abutting fiber. Increasing values of Q result in increasing peak strains in both the LE fragment and the abutting HE fiber. For values of $Q > 0.89$, no slip occurs, so the strain profiles are unchanging for $Q > 0.89$.

LOAD CONTRIBUTION OF LE FRAGMENTS

To obtain the total load on the unit cell, denoted f , we note that the total tension in each HE fiber in the unit cell is $E^*A^*(\varepsilon + du_{n,m}/dx)$, where the ε term occurs due to

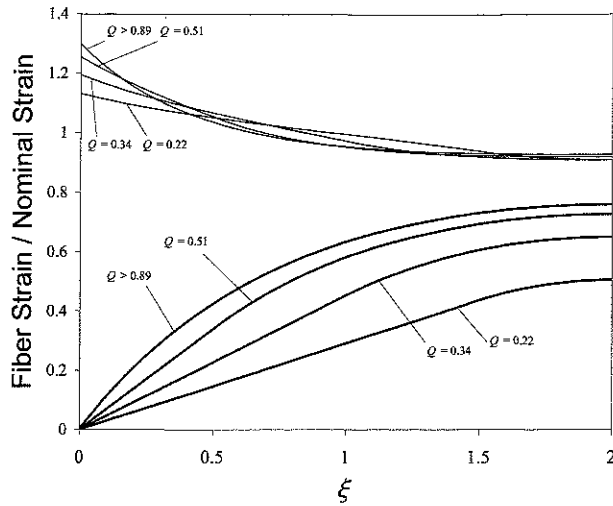


FIGURE 6. Fiber strain/nominal strain, $1 + U'_{n,m}$, versus position ξ for various Q . Thick line is LE fragment and thin line is the abutting HE fiber (1,0). $R = 1/3$, $k/k^* = 1$, and $L = 2$ for all cases.

the definition of the displacement reference. Evaluating the load on the unit cell at $\xi = 0$ simplifies matters, since the tension is zero on the LE fragment at the fragment tip. The total load f on the unit cell is computed by summing the HE fiber tensions at $\xi = 0$ for the $(2M + 1)^2 - 1$ HE fibers in the unit cell. Using Equations 3, f can be written as

$$f = E^*A^*\epsilon \sum_{\text{HE fibers}} \{U'_{n,m}(0) + 1\} \quad (19)$$

The total load f does not give a direct indication of the influence of the LE fragment, since f depends on the size of the unit cell, specified by M . The load contribution of the LE fragment f_{LE} is sought by subtracting out the effect of the HE fibers through the use of a comparison cell, where the LE fragment has been removed and its position left vacant. We note that the load on the comparison cell, denoted f_{HE} , is simply $E^*A^*\epsilon$ times the number of HE fibers in the unit cell. The load contribution of the LE fragment, defined by $f_{LE} = f - f_{HE}$, may be written, using Equation 19, as

$$f_{LE} = E^*A^*\epsilon \sum_{\text{HE fibers}} U'_{n,m}(0) \quad (20)$$

A convenient feature of f_{LE} is that its value is a direct measure of the effectiveness of the reinforcement provided by the fragments: when the value of f_{LE} falls below $E^*A^*\epsilon$, the fragmented blended fiber array carries less load at a given strain than an array consisting only of HE fibers.

The behavior of the LE fragment load contribution with increasing Q is exhibited in Figures 7 and 8 for

various fragment lengths. Results for various R are indicated in Figure 7, and those for various k/k^* are indicated in Figure 8. Here, for moderate or large values of Q , increasing the axial stiffness of the LE fragment (decreasing R) significantly increases the load contribution of the fragment, the effect becoming most pronounced for fragment lengths of two or greater. Increasing the stiffness of the shearing interaction between the LE fragment and the HE fiber (increasing k/k^*) for moderate or large values of Q also increases the fragment load contribution, but to a lesser extent than similar changes in axial stiffness. The effect of increases in the stiffness of the shearing interaction becomes most pronounced for shorter fragment lengths. For small values of Q , the LE fragment load contribution depends only on fragment length.

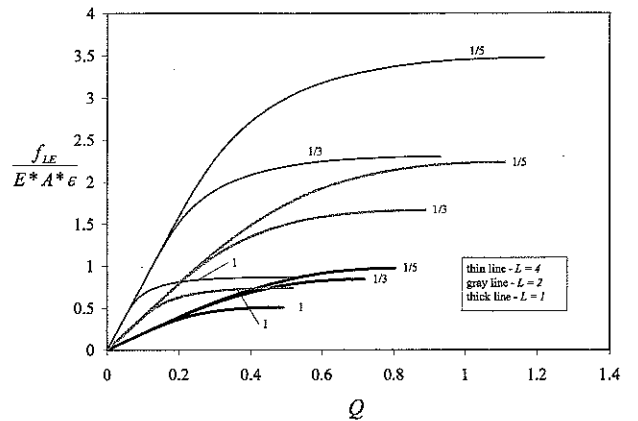


FIGURE 7. Load contribution of LE fragment for various fragment lengths and R values (shown next to curves). k/k^* is 1 for all cases.

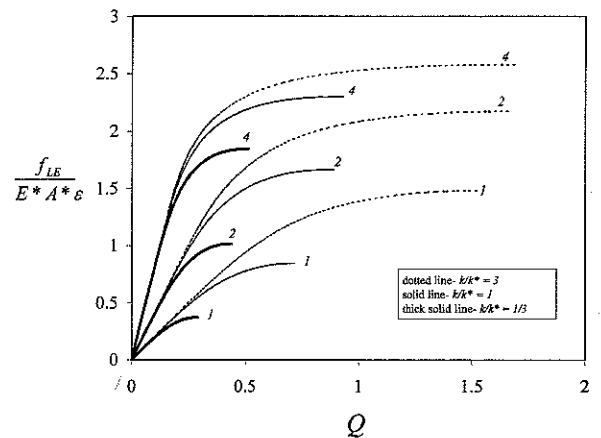


FIGURE 8. Load contribution of LE fragment for various fragment lengths and k/k^* values. Fragment length values L are shown next to curves. R is $1/3$ for all cases.

Discussion

We have investigated the post-fragmentation tensile behavior of twisted hybrid yarns containing a small fraction of LE fibers through a simple micromechanical model of a unit cell. Our results suggest that the dimensionless parameter Q has a critical influence on the degree to which behavior is governed by either elastic interaction or frictional slip between the LE fragment and surrounding HE fibers. The value of Q may therefore be a deciding factor in the success of particular hybrid yarn designs and approaches taken to improve yarn performance. Strategies intended to increase yarn stiffness and overall yarn tension during the fragmentation process by tailoring the elastic properties of the LE fibers, such as increasing LE fiber axial stiffness, will be ineffective if the prevailing Q values are too small, *i.e.*, such that behavior is dominated by frictional slip effects. When LE fibers are intended to significantly reinforce the yarn in the extension regime involving the LE fiber fragmentation process, the value of Q must be sufficiently high such that significant load transfer occurs between the fragment and surrounding HE fibers. Figures 7 and 8 show that yarn reinforcement by the LE fragments, requiring the fragmented blended fiber array to carry higher loads at a given strain than an all-HE fiber array (*i.e.*, $f_{LE} > E^*A^* \epsilon$), occurs for values of Q in the fiber array greater than, say, 0.2. For smaller values of Q , a homogeneous yarn consisting of only HE fibers would carry higher loads in the yarn extension regime associated with LE fiber fragmentation.

The helical fiber geometry resulting from yarn twist has an important influence over fragment slip behavior. In our model, slip frictional forces increase linearly with increasing strain, so increasing tension in the fiber fragment is balanced by increasing frictional forces. As a result, the extent of the slipping region remains constant with increasing strain. This is in contrast to models for fibrous composites exhibiting frictional fiber/matrix interfacial slip or matrix yielding near fiber breaks, where slip or matrix yield is assumed to occur at a constant stress. In those models, the extent of the slipping or matrix yield zone grows roughly linearly with increasing load (see, *e.g.*, reference 9). Consistent with the strain independence of the slip extent in our model, the parameter Q is also independent of the nominal strain in the fiber array, at least to a first-order approximation. In reality, Q is likely to be somewhat dependent on strain. As the yarn is extended, increases in the packing density of the fibers may bring additional fiber surfaces into contact, increasing frictional forces at a rate higher than in our model. This can be treated by considering the coefficient of friction to depend on the strain level in the

fiber array. For example, a judicious choice is $\mu = \mu_0 \epsilon^n$, where n is some positive fraction typically less than $1/2$, so that μ becomes asymptotic to a constant value at large strains as the packing density saturates.

We envision this model as a general framework to be used in a semi-empirical approach to the study of fragmentation and failure processes in hybrid yarns. As such, the critical parameter Q will ultimately be calibrated through appropriate experiments. Treating Q as a parameter to be calibrated is particularly prudent, because its definition in terms of microstructural properties, Equation 12, includes a fiber-to-fiber shearing stiffness k^* and the *in situ* coefficient of friction between HE and LE fiber surfaces. Both these quantities are likely to be tenuous, highly sensitive to the specifics of the yarn construction at hand, and so not quantities that can be independently measured.

It is worthwhile to use its definition to explore the likely values of Q as the fiber array properties are varied. If we assume both fibers are approximately the same diameter and are roughly circular in cross section, the quantity A^* is replaced by $\pi d^2/4$. The stiffness of the smeared fiber array, for fiber arrays with low concentrations of LE fibers, can be approximated by the stiffness of an array of all HE fibers, $\bar{E} \cong E^*A^*/d^2 \cong (\pi/4)E^*$. Making these substitutions into Equation 12, we find that $Q \cong \frac{1}{2} \pi^{1/2} \mu \eta \sqrt{E^*/k^*}$. This result suggests that increasing the ratio of HE fiber axial and fiber-to-fiber shearing stiffness, E^*/k^* , assuming yarn twist and frictional behavior is unchanged, will increase the value of Q within the yarn. Speculatively, HE fibers that have a more highly oriented molecular structure will tend to have higher E^*/k^* ratios and, other things being equal, will yield blended yarns with higher Q values. The dependence of Q on $\mu \eta$ is consistent with the familiar expectation that increasing the yarn twist (increasing η) will increase cohesiveness. Morton and Hearle [17, p. 419] tabulate the ratio of tensile to shear modulus for some common textile fibers. Using these values, which range from 3.2 for wool to 28 for a high-tenacity viscose rayon, as a rough estimate for E^*/k^* , taking $\mu = 0.3$ and $\eta = 0.18$, we may estimate Q values to be very roughly in the range of 0.1–0.3. For high performance fibers, Kevlar, for example, higher values of Q result (say, 0.4–0.7), since reported values of the tensile-to-shear modulus ratio are in the 100 to 200 range [11].

Conclusions

We have developed a simple micromechanical model for deformations in a fiber array representing the microstructure of a hybrid yarn undergoing fragmentation of the low elongation-to-break (LE) fibers during extension.

The model can be used as an initial framework in a semi-empirical approach to the study of hybrid yarn fragmentation and failure processes. The parallel square-stacked mixed array of elastic fibers consists of a small fraction of relatively high modulus, LE fibers dispersed among high elongation-to-break (HE) fibers. The LE fibers are assumed to break into fragments that slip relative to neighboring fibers in regions near the fragment tips; literature results for yarn internal stresses are used to motivate analysis of frictional slip forces. We use the model to investigate the contribution of the LE fragments to the load-carrying ability of the fiber array. Dimensionless parameters involving elastic and frictional properties of the fibers, properties of the fiber array, as well as yarn geometry are identified and their influence on hybrid yarn tensile behavior is discussed. A key parameter Q has a critical influence on the degree to which fiber array behavior is dominated by either elastic or frictional slip effects.

Literature Cited

1. Curtin, W. A., Theory of Mechanical Properties of Ceramic Matrix Composites, *J. Am. Ceram. Soc.* **74**, 2837–2845 (1991).
2. Curtin, W. A., The “Tough” to Brittle Transition in Brittle Matrix Composites, *J. Mech. Phys. Solids* **41**, 217–245 (1993).
3. Daniels, H. E., The Statistical Theory of Strength of Bundles of Threads, *Proc. R. Soc. Lond. A* **183**, 405–435 (1945).
4. Fukuda, H., and Chou, T. W., Stress Concentrations in a Hybrid Composite Sheet, *J. Appl. Mech.* **50**, 845–848 (1983).
5. Galilei, Galileo, “Dialogues Concerning Two New Sciences,” Leyden (1638), translated by A. De Salvio and A. Fabaro, Evanston, IL, 1914.
6. Godfrey, T. A., and Rossettos, J. N., The Onset of Tear Propagation at Slits in Stressed Uncoated Plain Weave Fabrics, *J. Appl. Mech.* **66**, 926–933 (1999).
7. Hearle, J. W. S., Grosberg, P., and Backer, S., “Structural Mechanics of Fibers, Yarns, and Fabrics,” Wiley-Interscience, NY, 1969.
8. Hedgepeth, J. M., Stress Concentrations in Filamentary Structures, NASA Technical Note D-882, 1961.
9. Hedgepeth, J. M., and Van Dyke, P., Local Stress Concentrations in Imperfect Filamentary Composite Materials, *J. Compos. Mater.* **1**, 294–309 (1967).
10. Hui, C.-Y., Phoenix, S. L., and Shia, D., Statistics of Fragmentation in a Single-Fiber Composite under Matrix Yielding and Debonding with Application to the Strength of Multi-Fiber Composites, *Compos. Sci. Technol.* **60**, 2107–2128 (2000).
11. Kawabata, S., “Measurements of Anisotropic Mechanical Property and Thermal Conductivity of a Single Fiber for Several High Performance Fibers,” presented at the Fourth Japan-U.S. Conference on Composite Materials, June 27–28, 1988, Washington, DC.
12. Kemp, A., and Owen, J. D., The Strength and Behaviour of Nylon/Cotton Blended Yarns Undergoing Strain, *J. Textile Inst.* **46**, T684–T698 (1955).
13. Kilby, W. F., The Mechanical Properties of Twisted Continuous-Filament Yarns, *J. Textile Inst.* **55**, T589–T632 (1964).
14. Manders, P. W., and Bader, M. G., The Strength of Hybrid Glass/Carbon Fibre Composites, Part 1: Failure Strain Enhancement and Failure Mode, *J. Mater. Sci.* **16**, 2233–2245 (1981).
15. Monego, C. J., The Mechanics of Rupture of Cotton-Dacron Yarns, Masters thesis, M.I.T., Cambridge, MA, 1963.
16. Monego, C. J., and Backer, S., Tensile Rupture of Blended Yarns, *Textile Res. J.* **38**, 762–766 (1968).
17. Morton, W. E., and Hearle, J. W. S., “Physical Properties of Textile Fibers,” Halsted Press, NY, 1975.
18. Neumeister, J. M., A Constitutive Law for Continuous Fiber Reinforced Brittle Matrix Composites with Fiber Fragmentation and Stress Recovery, *J. Mech. Phys. Solids* **41**, 1383–1404 (1993).
19. Pan, N., and Postle, R., The Tensile Strength of Hybrid Fibre Composites: A Probabilistic Analysis of the Hybrid Effects, *Phil. Trans. R. Soc. Lond. A* **354**, 1875–1897 (1996).
20. Phoenix, S. L., Statistical Theory for the Strength of Twisted Fiber Bundles with Applications to Yarns and Cables, *Textile Res. J.* **49**, 407–423 (1979).
21. Phoenix, S. L., Ibnabdeljalil, M., and Hui, C.-Y., Size Effects in the Distribution for Strength of Brittle Matrix Fibrous Composites, *Int. J. Solids Struct.* **34**, 545–568 (1996).
22. Pierce, F. T., Tensile Tests for Cotton Yarns, V: ‘The Weakest Link’ Theorems on the Strength of Long and of Composite Specimens, *J. Textile Inst.* **17**, 355 (1926).
23. Pitt, R. E., and Phoenix, S. L., On Modelling the Statistical Strength of Yarns and Cables Under Localized Load-Sharing Among Fibers, *Textile Res. J.* **51**, 408–425 (1981).
24. Realff, M. L., Pan, N., Seo, M., Boyce, M. C., and Backer, S., A Stochastic Simulation of the Failure Process and Ultimate Strength of Blended Continuous Yarns, *Textile Res. J.* **70**(5), 415–430 (2000).
25. Thwaites, J. J., The Elastic Deformation of a Rod with Helical Anisotropy, *Int. J. Mech. Sci.* **19**, 161–168 (1976).
26. Thwaites, J. J., A Continuum Model for Yarn Mechanics, in “Mechanics of Flexible Fibre Assemblies,” J. W. S. Hearle, J. J. Thwaites, and J. Amirbayat, Eds., Sijthoff & Noordhoff, Alphen aan den Rijn, The Netherlands, 1980, pp. 87–112.